RSF-1, A CHROMATIN REMODELING PROTEIN, INDUCES DNA DAMAGE AND PROMOTES GENOMIC INSTABILITY*

Jim Jinn-Chyuan Sheu[1,2], Bin Guan[1], Athena Lin[3], Chia-Huei Lee[4], Yi-Ting Hsiao[2], Fuu-Jen Tsai[2], Tian-Li Wang[1], and Ie-Ming Shih[1]

From Department of Pathology and Oncology, Johns Hopkins Medical Institutions, Baltimore, MD 21231, USA[1]; Human Genetic Center, China Medical University Hospital and School of Chinese Medicine, China Medical University, Taichung, 40447, Taiwan[2]; Department of Basic Sciences and International Health, Touro University, Vallejo, CA 94592, USA[3]; National Institute of Cancer Research, National Health Research Institutes, Miaoli, 35053, Taiwan[4]

Running head: Rsf-1 overexpression and DDRs

Address correspondence to: Ie-Ming Shih, MD, PhD, 1550 Orleans Street, Baltimore, MD21231. Tel: 410-502-7774; Fax: 410-502-7943; E-mail: ishih@jhmi.edu. And Jim Jinn-Chyuan Sheu, PhD, 2 Yuh Der Road, Taichung 40447, Taiwan. Tel: +886-4-22052121 ext.2037; Fax: +886-4-22053366; E-mail: jimsheu@mail.cmu.edu.tw.

***Rsf-1 (HBXAP)* has been reported as an amplified gene in human cancer including ovarian serous carcinoma, a highly aggressive disease in women. Rsf-1 protein interacts with SNF2H to form an ISWI chromatin remodeling complex, RSF. In this study, we investigated the functional role of Rsf-1 by observing the phenotypes after expressing Rsf-1 in non-transformed cells. Acute expression of Rsf-1 resulted in DNA damage as evidenced by DNA strand breaks, nuclear γH2AX foci and activation of the ATM-CHK2-p53-p21 pathway, leading to growth arrest and apoptosis. Deletion mutation and gene knockdown assays revealed that formation of a functional RSF complex with SNF2H was required for Rsf-1 to trigger DNA damage response. Gene knockout of *TP53* alleles, introduction of a dominant negative $TP53^{R175H}$, or treatment with an ATM inhibitor abolished upregulation of p53 and p21 and prevented Rsf-1-induced growth arrest. Chronic induction of Rsf-1 expression resulted in chromosomal aberration and clonal selection for cells with *Myc* amplification and *CDKN2A/B* deletion which are common in cancer. The above findings suggest that increased Rsf-1 expression and thus excessive RSF activity, as occurs in tumors harboring *Rsf-1* amplification, induces chromosomal instability likely through DNA damage response.**

Chromatin remodeling is a fundamental process in miscellaneous biological activities such as nucleotide synthesis, transcription regulation, DNA repair, methylation and recombination (1). The remodeling process is regulated by a group of nuclear protein complexes that assemble chromatin by sliding and spacing nucleosomes, allowing for accessibility of otherwise highly packaged DNA in the nucleosome to nuclear proteins including transcription factors, enhancers, repressors and enzymes. This process is made possible by the ATPase subunit of the chromatin remodeling complex which utilizes ATP hydrolysis to generate the energy needed to alter the chromatin architecture at the nucleosomal level. Two main classes of ATP-dependent chromatin remodeling complexes are identified and they include the ISWI (imitation switch) family and the SWI/SNF family, both of which are highly conserved in composition and function during evolution. ISWI complexes are able to move nucleosomes and alter their positions on DNA strands. Given the important roles of chromatin remodeling factors in biology, it comes as no surprise that defects in, or aberrant expression of, chromatin remodeling proteins are associated with a variety of diseases such as developmental disorders and cancer (2,3).

Using digital karyotyping, we have identified a discrete amplicon at chromosome (ch) 11q13.5 in ovarian high-grade serous carcinomas, a highly malignant neoplastic disease in women (4,5). This amplification was subsequently validated in two independent studies that profiled DNA copy number changes in ovarian carcinoma (5,6). In

addition to ovarian serous carcinoma, amplification at the ch11q13.5 region is also detected in other types of neoplastic diseases including breast, bladder, esophageal, and head and neck cancer (7). The minimal ch11q13.5 amplicon contains 13 genes; among them *Rsf-1* (*HBXAP*) showed the highest correlation between DNA and RNA copy number in ovarian cancer tissues (4) and was the only gene that contributed to drug resistance in ovarian cancer cells among amplified genes examined (8). We also observed that the amplification and overexpression of *Rsf-1* independently correlated with worse clinical outcomes in ovarian serous carcinoma patients, indicating the association of Rsf-1 and disease aggressiveness (4,9).

Molecularly, Rsf-1 protein partners with SNF2H through its DDT and PHD domains to form the RSF (Remodeling and Spacing Factor) complex that belongs to the ISWI chromatin remodeling gene family (10-13). It has been shown that SNF2H possesses nucleosome-dependent ATPase activity, while Rsf-1 (HBXAP) functions as a histone chaperone. As with other ISWI chromatin remodeling complexes, RSF has been reported to participate in nucleosome assembly and chromatin remodeling in response to a variety of growth signals and environmental cues (10-12). More recently, RSF has been shown to interact with centromere protein A (CENP-A) histone and it is essential to centromeric chromatin assembly complex formation (14). The protein level of Rsf-1 was correlated with that of SNF2H in human cancer tissues, and ectopic expression of Rsf-1 increased protein levels of SNF2H probably through formation of a stabilized RSF complex (13). *Rsf-1* gene knockdown or disruption of RSF complex formation inhibited cell growth in OVCAR3 ovarian cancer cells, which harbor *Rsf-1* amplification and thus express abundant endogenous Rsf-1, but not in other cancer cells without *Rsf-1* amplification or overexpression (8,13). These results strongly suggest that *Rsf-1* amplification is critical in maintaining the survival and growth in ovarian cancer cells.

In order to further determine the biological functions of Rsf-1 and its possible role in tumor development, we determined the effects by ectopic expression of Rsf-1 in non-transformed cells including an ovarian surface epithelial cell line and RK3E cells. Our findings suggest that excessive activity of chromatin remodeling through Rsf-1 overexpression, as occurs in tumor cells with *Rsf-1* amplification, can be detrimental to cells because of induction of DNA damage, resulting in growth arrest and apoptosis. However, in the presence of mutated p53, cells continue undergoing cell division despite DNA damage, thus promoting chromosomal instability as observed in cancer cells.

EXPERIMENTAL PROCEDURES

Establishment of Rsf-1 expressing cell models- To determine the effects of Rsf-1 expression, we transfected HEK293, NIH3T3, RK3E kidney epithelial cells, ovarian cancer cell lines including MPSC1 and SKOV3 cells, and ovarian surface epithelial cells with pcDNA6B-Rsf-1/V5 and attempted to select the clones in a selection medium containing G418 (150 μg/ml) (Calbiochem-Merck). Another immortalized ovarian surface epithelial cell line, IOSE80pc, was transduced by Rsf-1/V5 lentivirus (15) because the virus offered a more efficient system to deliver gene than transfection in this cell line. For the Rsf-1 inducible expression system, a full-length Rsf-1 gene and Rsf-1 deletion mutants tagged with V5 (C-terminal) were cloned into a Tet-off expression vector, pBI-EGFP (Clontech, Mountain View, CA). RK3E cells were transfected with the tetracycline-controlled transactivator (tTA) expression vector to generate RK3E-tTA cells. The inducible expression vectors were then introduced into the RK3E-tTA cells, and the stable transfectants were selected by hygromycin (Roche) and G418. For the retroviral delivery system, the coding sequence of Rsf-1/V5 was cloned into a retroviral vector, pWZL. The retroviral vectors were transfected into Phoenix retrovirus packaging cells and the virus particles were collected from the culture supernatant 2 days after transfection. Viral transduction was performed by incubating cells with viral supernatant overnight.

Cell growth, colony formation and apoptosis assays- Cells were grown in 96-well plates at a density of 3,000 cells per well. After overnight culture, the cells were washed with Dox-in (gene turned off) or Dox-free (gene turned on) medium, and the cell number was measured at different time points based on the fluorescence intensity of SYBR green I nucleic acid staining (Molecular

Probes, Eugene, OR). Cell growth was monitored daily for 4 consecutive days. For colony formation assay, cells were seeded in 25-cm^2 flasks at a cell density of 2,000 cells/flask with Dox-in or Dox-free medium. The colonies were counted after staining with crystal violet dye (Sigma) at day 10. To study the possible involvement of ATM kinase in mediating Rsf-1-induced cell death, RK3E cells were treated with 100nM or 200nM CGK733 (Merck Biosciences; Darmstadt, Germany). Cells treated with equal concentration of DMSO were used as the controls. For cell cycle analysis, both floating and attached cells were collected 24 hrs after gene expression for cell cycle analysis using the BD LSR1 flow cytometry (San Jose, CA). For apoptosis assay, apoptotic cells were detected by staining with Annexin V-FITC (BioVision, Mountain View, CA). The percentage of Annexin V (+) cells was determined by counting at least 400 cells from different fields for each experiment. The data was expressed as mean ± SD from triplicates.

DNA strand break assay- Quantification of DNA strand breaks was determined using a Comet assay kit (Trevigen, Inc., Gaithersburg, MD) (16). Rsf-1 expressing and non-expressing cells were harvested in ice-cold PBS at a density of 1×10^5 cells/mL. Cells treated with UV light at a sublethal dose were used as the positive control. Cells were mixed with LMAgarose at 1:10 ratio (v/v) and spread onto the CometSlide immediately. After gel solidification, the slides were inmmersed in an ice-cold lysis buffer provided by the kit for 45 min, followed by incubation in an alkaline solution provided by the kit at room temperature for one hour. The fragmented DNA strands were then separated from nuclei by electrophoresis and detected by SYBR Green staining. The percentage of comet-like nuclei (with DNA strand breaks) was counted under a fluorescence microscope from five randomly selected high-power fields (40X) with each approximately containing 100 nuclei.

Immunofluorescence staining- Rsf-1 transduced ovarian surface epithelium (OSE) cells were used to determine whether Rsf-1 expression resulted in genome instability. At different time points, cells on chamber slides were fixed with para-formaldehyde and incubated with anti-phospho-CHK2 (pCHK2) antibody (clone ab38461; Abcam, Cambridge, MA), anti-γH2AX antibody (clone ab11174; Abcam) for 2 hrs and followed by Rhodamin-conjugated anti-mouse or anti-rabbit antibody (Jackson ImmunoResearch Lab., West Grove, PA). Cell nuclei were counter stained with DAPI (Sigma).

G-banding karyotyping and abnormal mitosis counting- In order to assess if Rsf-1 expression resulted in an increase in chromosomal aberrations, we used an Rsf-1 inducible RK3E cell model in which Rsf-1 was repeatedly turned on for 3 passages then turned off for 3 passages to avoid growth arrest. After 10 cycles of repeated induction, cells were subject to G-banding karyotyping, array CGH and evaluation for abnormal mitotic figures. For G-banding karyotyping, cells were synchronized with 10 μg/ml colcemid (Invitorgen) for 3 hrs. Cells were then trypsinized and fixed with ice-cold fixation solution (methanol/glacial acetate = 3/1; vol/vol). After three times of wash with fixation buffer, the cell suspension was spotted onto slides air-dried slides, aged at 65 °C for 5 h or overnight and then were submitted to standard procedures of G-banding with trypsin. Images of ten metaphases in which there was minimal chromosome overlap, long chromosome length, little or no cytoplasm, and high banding resolution were selected for detailed analysis. Abnormal mitotic figures including spindle pole number abnormality, anaphase bridges and micronuclei was counted in approximately 400 randomly selected nuclei and the percentage was determined.

Array comparative genomic hybridization- A genome-wide oligonucleotide array with resolution of 35 kb (human genome CGH microarray 44B; Agilent Technologies, Palo Alto, CA) was used for array-CGH analysis. Genomic DNA fragmentation, labeling, and array hybridization were performed according to the standard protocol (version 4) provided by Agilent Technologies. DNA was isolated from long-term Rsf-1 turned on cells as the experimental genome and those isolated from Rsf-1 turned off or control cells of the same batch as the reference genome. The hybridized arrays were scanned using an Agilent G2565BA DNA microarray scanner and were analyzed using Agilent Feature Extraction software, version 8.1.1. Another custom analytical software package, Agilent CGH Analytics, version 3.4, was also used for the subsequent data analysis. The locations of the copy number aberations were

calculated using the *Z*-score statistical algorithm with a moving average window of 5 Mb. The *Z*-score threshold was set at 2.5 to make an amplification or deletion call. Based on these setting, the aberration score was generated automatically for each copy-number altered loci.

RESULTS

Rsf-1 expression induces growth arrest in cells with wild-type TP53. We have previously demonstrated that increasing Rsf-1 expression in ovarian cancer cells promotes tumor xenograft growth in mice (13). However, the immediate effects of Rsf-1 overexpression on non-transformed cells are not known. Here, we first expressed Rsf-1 in several cell lines that expressed low or undetectable levels of endogenous Rsf-1 by transfecting them with the pcDNA6B-Rsf-1/V5 expression vector. The cell lines included HEK293, NIH3T3, rat kidney epithelial cell line (RK3E), and an ovarian surface epithelial (OSE) cell culture which were non-transformed, non-tumorigenic and expressed wild-type *TP53*. SKOV3 cells, which harbored deleted*TP53* alleles, were used as the control. As compared to SKOV3, those *TP53* wild-type cell lines generated few, if any, colonies 6 weeks after transfection. To study the mechanism by which Rsf-1 expression led to growth suppression in those *TP53* wild-type cells, we selected an OSE cell line, a normal tissue counterpart of ovarian carcinoma, and a previously established Rsf-1 inducible cell line as the models. The RK3E cell line was used because it has been widely used to assess the transformational ability of potential oncogenes (17-22). Besides, we have previously generated RK3E-tTA clones for the Rsf-1 Tet-off inducible system which was difficult to be established in other cell lines mentioned above after several attempts.

We ectopically expressed Rsf-1 in IOSE80pc cells using an Rsf-1 expressing lentivirus and Rsf-1 expression was detected by Western blot analysis and by immunostaining (Fig. 1*A* and 1*B*). The IOSE80pc cell number was significantly reduced 4 days after transduction by Rsf-1/V5 lentivirus as compared to those transduced by control (vector only) virus (Fig. 1*C*). The apoptotic cells were increased in Rsf-1 expressing cells at Day 3 and Day 4 (Fig. 1*D*). For RK3E cells, we induced Rsf-1 expression by removing doxycyclin from culture medium. Based on Western blot analysis, we detected Rsf-1 protein expression in Rsf-1 Tet-off RK3E clones as early as 6 hours after induction (supplemental Fig. S1*A*). Furthermore, Rsf-1 co-immunoprecipitated with rat SNF2H (data not shown), indicating that ectopic Rsf-1 was able to interact with SNF2H to form the RSF chromatin remodeling complex in this cell line. As compared to the non-induced controls, Rsf-1 induced clones grew more slowly in culture, exhibited increased apoptotic activity when cells were incubated in a low-serum condition (0.5% FBS) based on Annexin V staining (supplemental Fig. S1*B*).

Rsf-1 induces DNA strand breaks and activates DNA damage responses. It has been established that oncogene can induce cellular senescence and cell death in pre-cancerous tissues by induction of DNA replication stress and activation of DNA damage responses (DDRs) (23-25). Thus, it is likely that Rsf-1 induction can also cause DDRs and subsequently growth arrest in those non-transformed cells with *TP53* wild type genetic background. To investigate this possibility, we measured protein levels of γH2AX, phosphorylated CHK2 (pCHK2), p53 and p21, all of which are involved in the DDR pathway, in both OSE cells (the IOSE80pc line) and RK3E Rsf-1 inducible cells. As shown in Fig. 2*A*, based on Western blot analysis OSE cells demonstrated increased protein levels not only of Rsf-1, but also of γH2AX, pCHK2, p53 and p21 six hours after Rsf-1 lentiviral transduction. Similarly, the same result in the expression pattern of Rsf-1, γH2AX, pCHK2, p53 and p21was observed in RK3E cells upon Rsf-1 induction (supplemental Fig. S2*A*). The above findings suggest that DNA strand breaks occur when Rsf-1 expression is induced. To determine if this was the case, we directly visualized DNA strand breaks in OSE cells transduced by Rsf-1/V5 and empty lentivirus, as well as in individual Rsf-1 induced and non-induced RK3E cells. Upon electrophoresis, DNA with strand breaks migrates out of nuclei forming a comet tail-like structure whereas non-damaged DNA remains within the nuclei. Fig. 2*B* and supplemental Fig. S2*B* show that a higher percentage of comet-like cells could be detected in the Rsf-1 expressing OSE cells and RK3E cells than in their control groups as early as 24 hrs after

Rsf-1 expression. At all time points, the percentage of comet-like cells was significantly higher in the Rsf-1 expressing cells than in the control cells. Immunofluorescence also showed concomitant γH2AX and pCHK2 foci in nuclei of OSE cells after Rsf-1 virus transduction (Fig. 2*C*) and in nuclei of RK3E cells after Rsf-1 induction (supplemental Fig.S2*C*).

For several oncogenes, the induced DDR by excessive oncogene products is always coupled with DNA replication (25). Therefore, we compared the ability to induce cell death, DNA strand breaks and micronuclei formation between dividing and confluent cells after Rsf-1 expression. Our result showed that Rsf-1-induced DDRs occur much more frequently in dividing cells than in confluent, non-dividing cells (Fig. 3), suggesting that replication was required for Rsf-1 induced DDR.

Inactivation of p53 or inhibition of ATM reverse the growth inhibitory effects by Rsf-1. The above results suggest that p53 is involved in the molecular check point for Rsf-1 induced DNA damage and subsequent DDR, and is responsible for growth arrest and apoptosis. Thus, it is likely that inactivation of p53 would abolish Rsf-1 induced growth suppression. To test this possibility, we performed two experiments by inactivating p53. First, when introduced to express a mutant p53 (R175H), Rsf-1 expressing RK3E cells were able to continue proliferating without causing apoptosis (supplemental Fig. S1*C*). Second, we ectopically expressed Rsf-1 in mouse embryonic fibroblasts (MEF) from three different genetic backgrounds ($MEF^{p53+/+}$, $MEF^{p53-/-}$ and $MEF^{ARF-/-}$) using the pWZL/Rsf-1 retrovirus. Similar to RK3E cells, $MEF^{p53+/+}$ responded to Rsf-1 expression by suppressing cell growth after two days (Fig. 4*A*). In contrast, $MEF^{p53-/-}$ (*TP53*-null) and $MEF^{ARF-/-}$ (*ARF*-null) cells did not show significant growth inhibition after Rsf-1 retrovirus transduction (Fig. 4*B* and 4*C*).

Since the DDR pathway is initiated by ATM/ATR activation upon DNA strand breaks, we further determined if the growth inhibitory effects induced by Rsf-1 overexpression could be abolished by ATM inactivation. We treated RK3E Rsf-1 inducible cells with an ATM kinase inhibitor, CGK733. Western blotting showed that the expression levels of p53 and p21, the DDR associated effectors, decreased by CGK733 treatment despite Rsf-1 was successfully turned on (Fig. 5*A*). Based on growth curve analysis and colony numbers, we found that the inhibitor was able to reverse the growth suppression effect conferred by Rsf-1 (Fig. 5*B* and 5*C*). The above findings supported that ATM and p53 were responsible for Rsf-1 induced growth suppression.

Formation of functional RSF complex is required for Rsf-1 to induce growth arrest. Because Rsf-1 interacts with SNF2H to form the RSF chromatin remodeling complex, here we asked if this interaction is required for Rsf-1-induced growth arrest. SNF2H siRNA was used to suppress SNF2H expression which resulted in reduced expression levels of γH2AX and pCHK2 (Fig. 6*A*). Western blot analysis revealed the effectiveness of the siRNA to down-regulate the SNF2H expression in treated cells (Fig. 6*B*). We found that more than 85% cells were negative for γH2AX after SNF2H knockdown, whereas 57% of cells were negative for pCHK2 after SNF2H knockdown (Fig. 6*C*). Notably, SNF2H knockdown partially rescued Rsf-1-induced growth arrest (Fig. 6*D*) indicating that the interaction between Rsf-1 with SNF2H is required for growth arrest.

Our previous study indicated that the DDT and PHD domains on Rsf-1 were essential for the protein to interact with SNF2H (13). Here we determined whether the SNF2H binding motif in Rsf-1 containing both DDT and PHD domains was sufficient to induce growth arrest. To this end, we generated RK3E clones with a Tet-off inducible expression system for several Rsf-1 deletion mutants including Rsf-D1 (1-441 a.a.), Rsf-D3 (1-871 a.a.), D4 (1-973 a.a.) and D6 (982-1441 a.a.) (Fig. 6*E* and 6*F*). Of note, Rsf-D4 represented the minimal fragment of Rsf-1 that interacted with SNF2H. Interestingly, we did not observe significant growth inhibitory or apoptosis-enhancing effects in all clones expressing these deletion constructs, including the Rsf-D4 construct (Fig. 6*G*). This observation suggested that both full length Rsf-1 and SNF2H were required to form a functional RSF complex which was responsible for the growth suppression effects.

Chronic Rsf-1 induction results in chromosomal instability. DNA damage in excess of repair capacity has been shown to contribute to genomic instability and provide a mixture of

genetically heterogeneous clones for Darwinian selection, thus propelling tumor development (23). To investigate the prolonged effect of Rsf-1 induction and assess its role in a biological context in non-transformed cells, we repeated turning on and off the Rsf-1 expression periodically to prevent acute growth arrest and apoptosis. Here, we determined whether or not genomic alterations were increased in Rsf-1 inducible RK3E cells which allowed us to manipulate Rsf-1 expression *in vitro*. The level of chromosomal aberration was determined by the percentage of abnormal mitosis, karyotypic aberration, and DNA copy number changes by comparing the Rsf-1 expressing cells to the control cells. First, we found that Rsf-1 induction increased the percentage of cells with abnormal mitoses including increased numbers of micronuclei, increased numbers of anaphase bridges, and increased numbers of mitotic spindle poles (Fig. 7*A*). Second, we found that Rsf-1 expression promoted karyotypic aberrations including gain and loss of whole and partial chromosomal arms, and gain of aberrant chromosomes that could not be assigned to specific chromosomes (Fig. 7*B* and 7*C*). In order to identify genome wide DNA copy number alterations associated with Rsf-1 expression, we performed array comparative genomic hybridization and compared the profiles among Rsf-1 induced, Rsf-1 non-induced, and mock induced (vector alone) RK3E cells (Fig. 7*D*). There were no differences in DNA copy number changes between Rsf-1 non-induced cells and mock induced cells. In contrast, clonal amplifications and deletions in discrete regions were detected in Rsf-1 induced cells as compared to either Rsf-1 non-induced cells or mock induced cells. The most pronounced changes included amplification at ch7q31 to ch7q33 (94,580,952-104,649,976), which harbors *c-Myc* and homozygous deletion at ch5q31 to ch5q34 (108,138,927-130,524,001), which contains *CDKN2A/B*.

DISCUSSION

Remodeling chromatin structure is essential for several critical nuclear functions, and aberrant activity in chromatin remodeling emerges as a contributor to tumor development. Our previous studies established the clinical significance and the essential role of Rsf-1 for cell survival in ovarian cancer. Here, we investigate the biological effects of Rsf-1 in non-tumorigenic cells and demonstrate that Rsf-1 expression induces chromosomal aberration through unchecked DNA damage response. We found that Rsf-1 expression was associated with growth arrest in cells unless they harbored mutant *TP53*, suggesting that *TP53* mutation is a prerequisite for Rsf-1 to promote tumor progression. Ectopic Rsf-1 expression in cells expressing wild-type *TP53* resulted in DNA strand breaks and subsequent activation of the ATM-pCHK2-p53-p21 DDR pathway followed by growth inhibition and apoptosis. Introduction of mutant p53 proteins or ATM inhibitor abrogated the Rsf-1-induced cell growth arrest. We further demonstrated that excessive Rsf-1 protein enhanced chromosomal instability, probably as a result of Rsf-1-induced DNA strand breaks. The findings from this study provide a new insight into the role of ISWI chromatin remodeling and cancer.

The observations made in this study have several biological implications. Initiation of DDR response by Rsf-1 overexpression is unique in chromatin remodeling complexes reported to date. This finding is similar to observations made in non-transformed cells after ectopic expression of certain oncogenes (24,26,27). Because the DDR pathway could be activated in the absence of actual DNA damage (28), it is possible that an increased level of Rsf-1, as occurs in *Rsf-1* amplified cancer cells, may trigger a false signal as if DNA damage had occurred. However, our results using the cell DNA electrophoresis assay clearly showed that Rsf-1 induction, similar to UV irradiation, in chromosomally stable OSE and RK3E cells caused DNA strand breaks. The mechanism by which an excessive amount of Rsf-1 proteins contributes to DNA strand breaks is intriguing. The finding that the Rsf-1-induced DDR depended on SNF2H suggests that the formation of the Rsf-1/SNF2H complex, and by inference, chromatin remodeling activity, is essential to mediate this effect. Paradoxically, ATP-dependent chromatin remodeling complexes have been demonstrated to play a critical role in the repair of DNA double-strand breaks. These complexes are recruited to DNA damaged sites and are directly involved in both homologous recombination and non-homologous end-joining repair (29). Specifically, certain

chromatin-remodeling complexes function by exchanging histone dimer pairs within nucleosomes, thereby re-shaping the landscape with histones bearing different modifications, which in turn serve as a molecular "bar code" to recruit specific nuclear factors for DNA damage repair (30,31). It can be envisioned that an increased Rsf-1 protein level accelerates or stabilizes the formation of the RSF chromatin remodeling complex.

Although an appropriate level of chromatin remodeling activity is essential for DNA repair, excessive RSF chromatin remodeling complexes could directly or indirectly compromise the repair system leading to cumulative DNA strand breaks. This view is supported by previous reports showing that overexpression of Rad51 recombinase, which is essential for homologous recombination and repair of DNA double strand breaks, leads to DNA double strand breaks and chromosomal instability as evidenced by exaggerated recombination events including chromosomal translocations, multiple chromosomal rearrangements, and aneuploidy (32,33). As DNA damage frequently occurs in cancer cells, probably because of enhanced oxidative stress, Rsf-1 overexpression may compromise DNA repair efficiency and subsequently leads to unrepaired DNA damage.

The above represents our favored view, but alternative mechanisms should also be pointed out. Excessive Rsf-1 proteins sequester SNF2H and alter subcellular distribution and partnership of SNF2H. Besides Rsf-1, SNF2H interacts with several other cellular proteins, and the SNF2H containing ISWI complexes are known to have diverse cellular functions including DNA repair (30,34). Thus, excessive Rsf-1 molecules may compromise the formation of other SNF2H containing chromatin remodeling complexes involving DNA repair. Indeed, it has been reported that inhibition of expression of SNF2 led to activation of DNA damage response pathway, growth inhibition and cell cycle G2M arrest (35), similar to the phenotypes induced by ectopic expression of Rsf-1.

The current results imply that a mechanism has evolved to protect normal cells from exaggerated chromatin remodeling and subsequent DNA damage in response to Rsf-1 overexpression. How do tumor cells overcome the growth inhibitory effect due to Rsf-1 amplification? As occurs in oncogenic stress, increased p53 levels due to the ATM-pCHK2-p53-p21 pathway activation lead to cell growth arrest at G1 or G2/M and/or to apoptosis (36). This negative selection pressure has the effect on clonally selecting tumor cells with defective p53. Indeed, using ovarian cancer as a disease model, we demonstrated that all 23 ovarian serous carcinomas with Rsf-1 overexpression harbored *TP53* mutations (data not shown), a finding similar to a previous transgenic mouse study showing frequent inactivating mutations of *TP53* in transgenic Myc-induced lymphomas (37). Therefore, the cooperation between *TP53* tumor suppressor and tumor-promoting genes as observed *in vitro* may likely occur in tumor tissues.

Consistent with this view, our recent study has shown that *TP53* mutation may likely precede *Rsf-1* gene upregulation in the development of ovarian cancer (38). Moreover, our results demonstrate that introduction of a mutant *TP53* gene into $TP53^{wt}$ cells, or knockout of *TP53* alleles, rescues cells from Rsf-1-induced growth arrest. Collectively, these results indicate that inactivation of p53 abolishes the checkpoint governed by the ATM-p53 pathway and allows cells to continue proliferating despite the presence of DNA damage. Such unchecked DNA damage is associated with accumulation of chromosomal aberrations in dividing cells, creating a repertoire of genetically heterogeneous tumor cell species, some of which further evolve under host selection pressures leading to clonal outgrowth of tumor cells with specific genetic changes. Toward this end, we found that overexpression of Rsf-1 promoted chromosomal instability as evidenced by increased karyotypic abnormalities and DNA copy number alterations in otherwise chromosomally stable cells. Chromosomal instability has been known as a hallmark of neoplastic diseases and its causal roles in tumor development can be demonstrated in certain types of cancer (39). For example, induction of aneuploidy by overexpression of the cysteine protease separase was associated with mammary tumorigenesis (40). Our finding that Rsf-1 induction in non-transformed cells is associated with *Myc* amplification and *CDKN2A/2B* homozygous deletion argues that such clonal selection exists in our experimental

system because both molecular genetic events are frequently detected in human carcinomas.

In summary, the current study demonstrates the biological effects of Rsf-1 overexpression as occurs in tumors harboring *Rsf-1* gene amplification in non-transformed cells. Excessive Rsf-1 proteins and probably increased RSF chromatin remodeling activity induce DNA strand breaks, activate the ATM/p53-dependent DNA damage response and lead to growth arrest and apoptosis in cells with wild-type *TP53*. Defective p53 as present in almost all ovarian serous carcinomas lifts the p53 DNA damage checkpoint, allowing tumor cells to proliferate in the presence of DNA strand breaks resulting in chromosomal aberrations. The findings reported here suggest an alternative mechanism in developing chromosomal instability in ovarian tumor cells and provide a new avenue for future studies aimed at elucidating the roles of chromatin remodeling in cancer.

REFERENCES

1. Ho, L., and Crabtree, G. R. (2010) *Nature* **463**(7280), 474-484
2. Wolffe, A. P. (2001) *Oncogene* **20**(24), 2988-2990
3. Lafon-Hughes, L., Di Tomaso, M. V., Mendez-Acuna, L., and Martinez-Lopez, W. (2008) *Mutat Res* **658**(3), 191-214
4. Shih Ie, M., Sheu, J. J., Santillan, A., Nakayama, K., Yen, M. J., Bristow, R. E., Vang, R., Parmigiani, G., Kurman, R. J., Trope, C. G., Davidson, B., and Wang, T. L. (2005) *Proc Natl Acad Sci U S A* **102**(39), 14004-14009
5. Nakayama, K., Nakayama, N., Jinawath, N., Salani, R., Kurman, R. J., Shih Ie, M., and Wang, T. L. (2007) *Int J Cancer* **120**(12), 2613-2617
6. Brown, L. A., Kalloger, S. E., Miller, M. A., Shih Ie, M., McKinney, S. E., Santos, J. L., Swenerton, K., Spellman, P. T., Gray, J., Gilks, C. B., and Huntsman, D. G. (2008) *Genes Chromosomes Cancer* **47**(6), 481-489
7. Schwab, M. (1998) *Bioessays* **20**(6), 473-479
8. Choi, J. H., Sheu, J. J., Guan, B., Jinawath, N., Markowski, P., Wang, T. L., and Shih Ie, M. (2009) *Cancer Res* **69**(4), 1407-1415
9. Davidson, B., Trope, C. G., Wang, T. L., and Shih Ie, M. (2006) *Gynecol Oncol* **103**(3), 814-819
10. LeRoy, G., Loyola, A., Lane, W. S., and Reinberg, D. (2000) *J Biol Chem* **275**(20), 14787-14790
11. Loyola, A., Huang, J.-Y., LeRoy, G., Hu, S., Wang, Y.-H., Donnelly, R. J., Lane, W. S., Lee, S.-C., and Reinberg, D. (2003) *Mol. Cell. Biol.* **23**(19), 6759-6768
12. Loyola, A., LeRoy, G., Wang, Y. H., and Reinberg, D. (2001) *Genes Dev* **15**(21), 2837-2851
13. Sheu, J. J., Choi, J. H., Yildiz, I., Tsai, F. J., Shaul, Y., Wang, T. L., and Shih, I. M. (2008) *Cancer Res* **68**(11), 4050-4057
14. Perpelescu, M., Nozaki, N., Obuse, C., Yang, H., and Yoda, K. (2009) *J Cell Biol* **185**(3), 397-407
15. Choi, J. H., Park, S. H., Leung, P. C., and Choi, K. C. (2005) *J Clin Endocrinol Metab* **90**(1), 207-210
16. Singh, N. P., McCoy, M. T., Tice, R. R., and Schneider, E. L. (1988) *Exp Cell Res* **175**(1), 184-191
17. Kolligs, F. T., Hu, G., Dang, C. V., and Fearon, E. R. (1999) *Mol Cell Biol* **19**(8), 5696-5706
18. Hendrix, N. D., Wu, R., Kuick, R., Schwartz, D. R., Fearon, E. R., and Cho, K. R. (2006) *Cancer Res* **66**(3), 1354-1362
19. Komiya, T., Park, Y., Modi, S., Coxon, A. B., Oh, H., and Kaye, F. J. (2006) *Oncogene* **25**(45), 6128-6132
20. Bommer, G. T., Jager, C., Durr, E. M., Baehs, S., Eichhorst, S. T., Brabletz, T., Hu, G., Frohlich, T., Arnold, G., Kress, D. C., Goke, B., Fearon, E. R., and Kolligs, F. T. (2005) *J Biol Chem* **280**(9), 7962-7975
21. Foster, K. W., Ren, S., Louro, I. D., Lobo-Ruppert, S. M., McKie-Bell, P., Grizzle, W., Hayes, M. R., Broker, T. R., Chow, L. T., and Ruppert, J. M. (1999) *Cell Growth Differ* **10**(6), 423-434
22. Kolligs, F. T., Nieman, M. T., Winer, I., Hu, G., Van Mater, D., Feng, Y., Smith, I. M., Wu, R., Zhai, Y., Cho, K. R., and Fearon, E. R. (2002) *Cancer Cell* **1**(2), 145-155

23. Bartkova, J., Horejsi, Z., Koed, K., Kramer, A., Tort, F., Zieger, K., Guldberg, P., Sehested, M., Nesland, J. M., Lukas, C., Orntoft, T., Lukas, J., and Bartek, J. (2005) *Nature* **434**(7035), 864-870
24. Bartkova, J., Rezaei, N., Liontos, M., Karakaidos, P., Kletsas, D., Issaeva, N., Vassiliou, L. V., Kolettas, E., Niforou, K., Zoumpourlis, V. C., Takaoka, M., Nakagawa, H., Tort, F., Fugger, K., Johansson, F., Sehested, M., Andersen, C. L., Dyrskjot, L., Orntoft, T., Lukas, J., Kittas, C., Helleday, T., Halazonetis, T. D., Bartek, J., and Gorgoulis, V. G. (2006) *Nature* **444**(7119), 633-637
25. Bartek, J., Bartkova, J., and Lukas, J. (2007) *Oncogene* **26**(56), 7773-7779
26. Di Micco, R., Fumagalli, M., Cicalese, A., Piccinin, S., Gasparini, P., Luise, C., Schurra, C., Garre, M., Nuciforo, P. G., Bensimon, A., Maestro, R., Pelicci, P. G., and d'Adda di Fagagna, F. (2006) *Nature* **444**(7119), 638-642
27. Di Micco, R., Fumagalli, M., and d'Adda di Fagagna, F. (2007) *Trends Cell Biol* **17**(11), 529-536
28. Soutoglou, E., and Misteli, T. (2008) *Science* **320**(5882), 1507-1510
29. Bao, Y., and Shen, X. (2007) *Curr Opin Genet Dev* **17**(2), 126-131
30. Wang, G. G., Allis, C. D., and Chi, P. (2007) *Trends Mol Med* **13**(9), 373-380
31. Downey, M., and Durocher, D. (2006) *Nat Cell Biol* **8**(1), 9-10
32. Richardson, C., Stark, J. M., Ommundsen, M., and Jasin, M. (2004) *Oncogene* **23**(2), 546-553
33. Francis, R., and Richardson, C. (2007) *Genes Dev* **21**(9), 1064-1074
34. Xiao, A., Li, H., Shechter, D., Ahn, S. H., Fabrizio, L. A., Erdjument-Bromage, H., Ishibe-Murakami, S., Wang, B., Tempst, P., Hofmann, K., Patel, D. J., Elledge, S. J., and Allis, C. D. (2009) *Nature* **457**(7225), 57-62
35. Ye, Y., Xiao, Y., Wang, W., Wang, Q., Yearsley, K., Wani, A. A., Yan, Q., Gao, J. X., Shetuni, B. S., and Barsky, S. H. (2009) *Mol Cancer Res* **7**(12), 1984-1999
36. Vogelstein, B., Lane, D., and Levine, A. J. (2000) *Nature* **408**(6810), 307-310
37. Eischen, C. M., Weber, J. D., Roussel, M. F., Sherr, C. J., and Cleveland, J. L. (1999) *Genes Dev* **13**(20), 2658-2669
38. Sehdev, A. S., Kurman, R. J., Kuhn, E., and Shih, I.-M. (2010) *Mod Pathol* **in press**
39. Weaver, B. A., and Cleveland, D. W. (2006) *Curr Opin Cell Biol* **18**(6), 658-667
40. Zhang, N., Ge, G., Meyer, R., Sethi, S., Basu, D., Pradhan, S., Zhao, Y. J., Li, X. N., Cai, W. W., El-Naggar, A. K., Baladandayuthapani, V., Kittrell, F. S., Rao, P. H., Medina, D., and Pati, D. (2008) *Proc Natl Acad Sci U S A* **105**(35), 13033-13038.

FOOTNOTES

*The authors thank Dr. T. L. Mao and Dr. A. Ayhan for their assistance with the *TP53* sequencing analysis, David Chu for his technical assistance, and Dr. J. Y. Chen (National Health Research Institute, Taiwan) for his critical suggestions. This work was supported by NIH/NCI grants (RO1CA129080, RO1CA103937), Johns Hopkins-China Medical University Research Collaboration Fund (DMR-98-104), and a NSC grant (NSC 98-2320-B-039-033-MY3) in Taiwan.

The abbreviations used are: ISWI, imitation switch; HBXAP, hepatitis B virus X protein associated protein; RSF, Remodeling and Spacing Factor; OSE, ovarian surface epithelium; DDR, DNA damage response.

FIGURE LEGENDS

Fig.1. Rsf-1 expression induces growth arrest in cells with wild-type *TP53*. IOSE80pc cells were used for studying the biological effects induced by Rsf-1 overexpression. *A*, Western blot shows Rsf-1-V5 protein band in cells transduced with a lentivirus expressing Rsf-1-V5 by using an anti-V5 antibody. *B*, immunocytochemistry demonstrates nuclear Rsf-1-V5 immunoreactivity in almost all Rsf-1-V5 transduced cells. *C*, cell growth analysis demonstrated a growth arrest in Rsf-1-V5 virus-transduced IOSE80pc cells as compared to control virus-transduced cells. *D*, the percentage of Annexin V stained

apoptotic cells increased in Rsf-1 virus-transduced cells as compared to control virus-transduced cells at day 3 and day 4 after virus transduction ($p < 0.001$).

Fig. 2. Rsf-1 induces DNA strand breaks and activates DNA damage response. IOSE80pc cells were used for studying the DNA damage response induced by Rsf-1 overexpression. *A*, Western blot analysis showed that Rsf-1 overexpression in ovarian surface epithelial cells was associated with increased protein levels of phosphorylated γ-histone 2AX (γH2AX), phosphorylated check point kinase-2 (pCHK2), p53, and p21. GAPDH serves as a loading control. *B*, upon gel electrophoresis, DNA with strand breaks migrated out of nuclei forming a comet tail like structure whereas the non-damaged DNA remained stationary within the nucleus. At all time points, the percentage of comet-like cells was significantly higher in the Rsf-1 overexpressing group than in the control group ($p < 0.001$). Ultraviolet light-irradiated cells (UV) serve as the positive control. *C*, immunofluorescence staining demonstrates punctuate immunofluorescence (foci) of both γH2AX and pCHK2 in cells at 36 hrs and 48 hrs after Rsf-1 transduction.

Fig. 3. Comparisons of the Rsf-1-induced effects on dividing cells and confluent cells. *A*, after Rsf-1 induction, immunofluorescence staining demonstrates formation of both γH2AX and pCHK2 foci in cells undergoing diving, but not in confluent cells. *B*, cell growth assay indicated less cell death in confluent cells after Rsf-1 induction. *C*, less DNA breaks were also found when Rsf-1 was turned on in confluent cells. *D*, less micronuclei were found when Rsf-1 was turned on in confluent cells.

Fig. 4. Defects in *TP53* and *ARF* reverse Rsf-1-induced cell growth arrest. The effects of Rsf-1 expression were tested on mouse embryonic fibroblast (MEF) with different genetic background. *A*, Western blot analysis shows Rsf-1 protein expression in pWZL-Rsf-1 retrovirus transduced MEF but not in the control virus (pWZL vector only) transduced cells. GAPDH was used as the loading control. After virus transduction, MEF with $TP53^{wt}$ showed a remarkable growth inhibition at day 6. *B*, MEF cells with different genetic backgrounds were transduced with pWZL-Rsf-1 retrovirus. In contrast to $TP53^{wt}$, MEF with *TP53* null and *Arf* null continued to grow after virus transduction. *C*, Phase contrast images show the cell number in Rsf-1 transduced $TP53^{wt}$ MEF was significantly reduced as compared to *TP53* null and *Arf* null MEF.

Fig. 5. ATM inactivation suppresses Rsf-1-induced cell growth arrest. *A*, ATM inhibitor, CGK733, (100 nM) abolishes Rsf-1-induced upregulation of p53 and p21 proteins in the Western blot. Of note, p21 protein level was very low but detectable. *B*, growth curves analysis demonstrates that CGK733 prevents growth arrest in RK3E cells after Rsf-1 induction. *C*, CGK733 at 100 nM and 200 nM rescued Rsf-1-induced growth suppression as the colony number increased as compared to 0 nM ($p < 0.001$).

Fig. 6. Interaction of full-length Rsf-1 and SNF2H is required for Rsf-1 to induce growth arrest in *TP53* wild type cells. *A*, most of SNF2H knockdown cells exhibited undetectable staining of pCHK2 and γH2AX. *B*, Western blot analysis showed an efficient reduction of SNF2H protein by SNF2H specific siRNA. *C*, co-events were those cells with down regulation of both SNF2H and pCHK2 or both SNF2H and γH2AX. *D*, growth curve analysis in Rsf-1 inducible RK3E cells transfected with anti-SNF2H or control siRNA. *E*, schematic presentation of full-length Rsf-1 and its different deletion mutants (D1, D3, D4 and D6). *F*, Western blot analysis showed expression of deletion mutants in RK3E cells 48 hrs after induction. *G*, growth curve analysis demonstrates no significant effects of deletion mutants on cellular proliferation as compared to full-length Rsf-1.

Fig. 7. Chronic Rsf-1 induction leads to chromosomal abnormality. *A*, the frequency of abnormal mitoses including micronuclei, abnormal spindle pole number and anaphase bridge increases in the Rsf-1 induced RK3E cells (filled symbols) as compared to the non-induced control cells (open symbols) at different time

points. *B*, karyotypic analysis demonstrates different types of gross karyotypic abnormality in Rsf-1 induced cells. *C*, examples of karyotypes in Rsf-1 induced (Rsf-1 on) and non-induced (Rsf-1 off) cells. *D*, array CGH showed clonal DNA copy number alterations including deletion in ch5, ch7 and ch9, and amplification in ch7 in RK3E cells after Rsf-1 induction whereas the Rsf-1 non-induced and mock induced RK3E (vector only control) cells displayed no such changes.

Figure 1

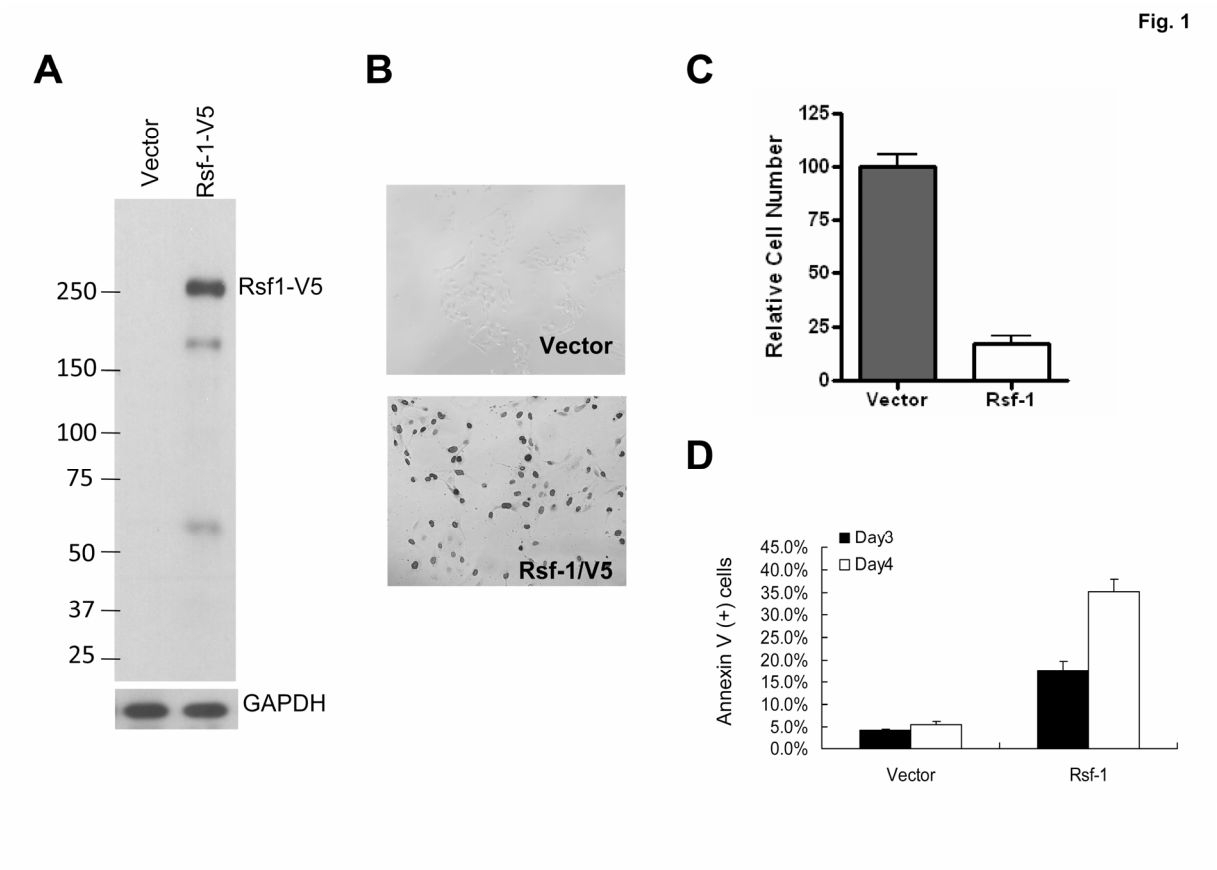
Fig. 1
A
Vector
Rsf-1-V5
250
150
100
75
50
37
25
Rsf1-V5
GAPDH
B
Vector
Rsf-1/V5
C
Relative Cell Number
125
100
75
50
25
0
Vector
Rsf-1
D
Annexin V (+) cells
Day3
Day4
45.0%
40.0%
35.0%
30.0%
25.0%
20.0%
15.0%
10.0%
5.0%
0.0%
Vector
Rsf-1

Figure 2

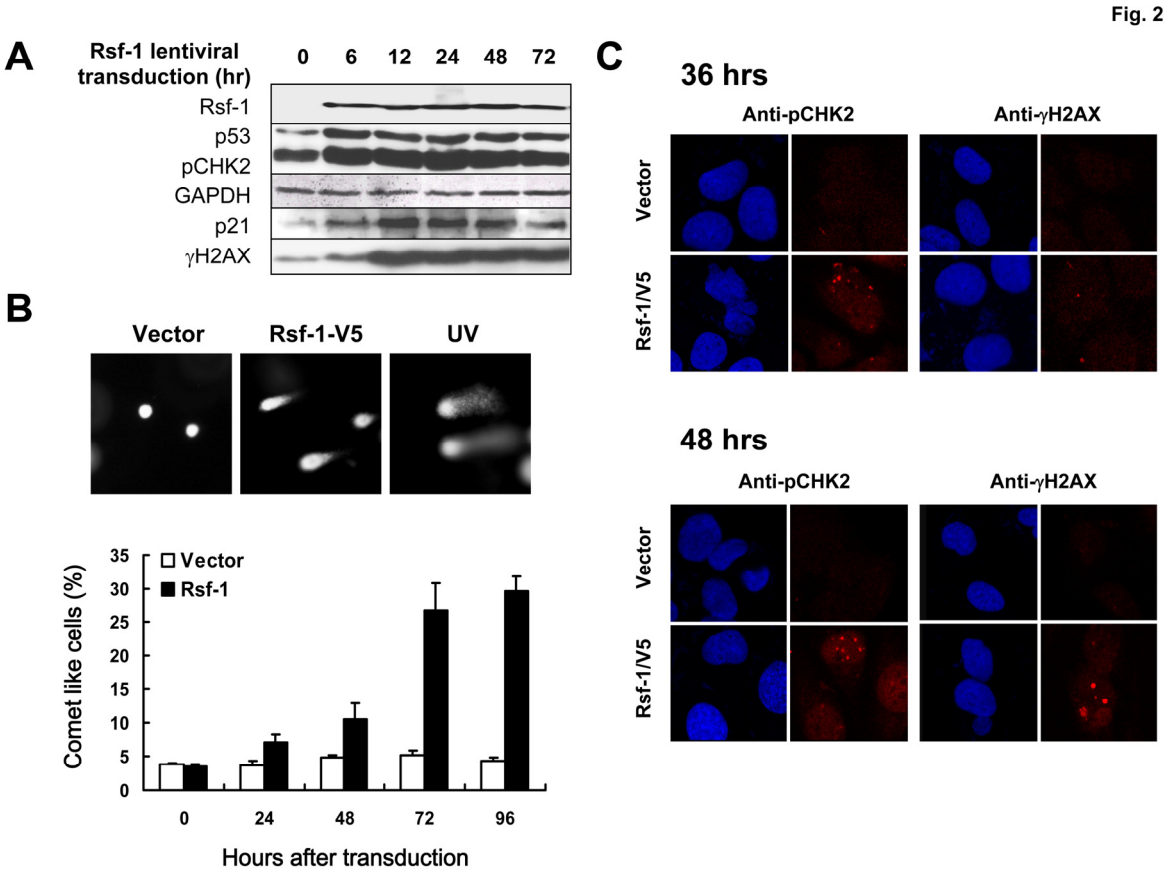
Fig. 2
A
Rsf-1 lentiviral transduction (hr)
0 6 12 24 48 72
Rsf-1
p53
pCHK2
GAPDH
p21
γH2AX
B
Vector
Rsf-1-V5
UV
Comet like cells (%)
Vector
Rsf-1
35
30
25
20
15
10
5
0
0 24 48 72 96
Hours after transduction
C
36 hrs
Anti-pCHK2
Anti-γH2AX
Vector
Rsf-1/V5
48 hrs
Anti-pCHK2
Anti-γH2AX
Vector
Rsf-1/V5

Figure 3

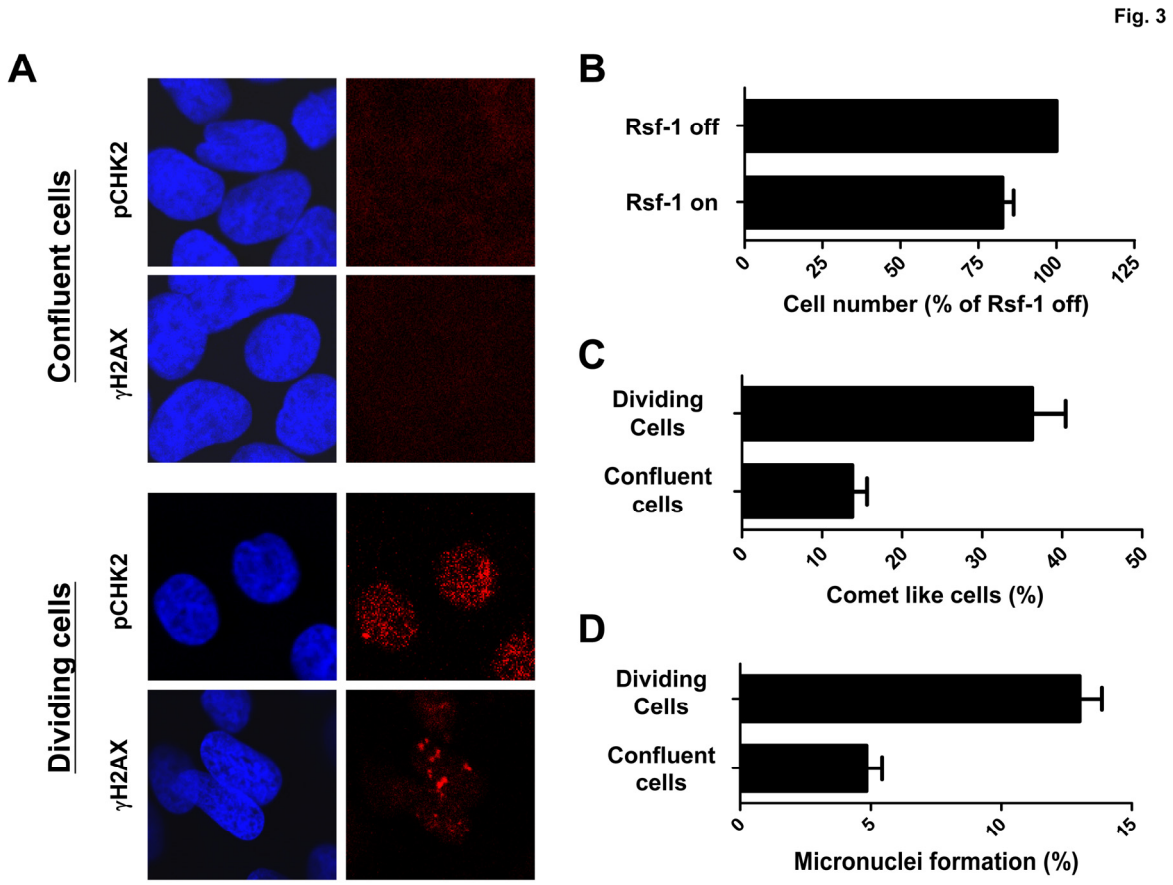
Fig. 3
A
Confluent cells
pCHK2
γH2AX
Dividing cells
pCHK2
γH2AX
B
Rsf-1 off
Rsf-1 on
0
25
50
75
100
125
Cell number (% of Rsf-1 off)
C
Dividing Cells
Confluent cells
0
10
20
30
40
50
Comet like cells (%)
D
Dividing Cells
Confluent cells
0
5
10
15
Micronuclei formation (%)

Figure 4

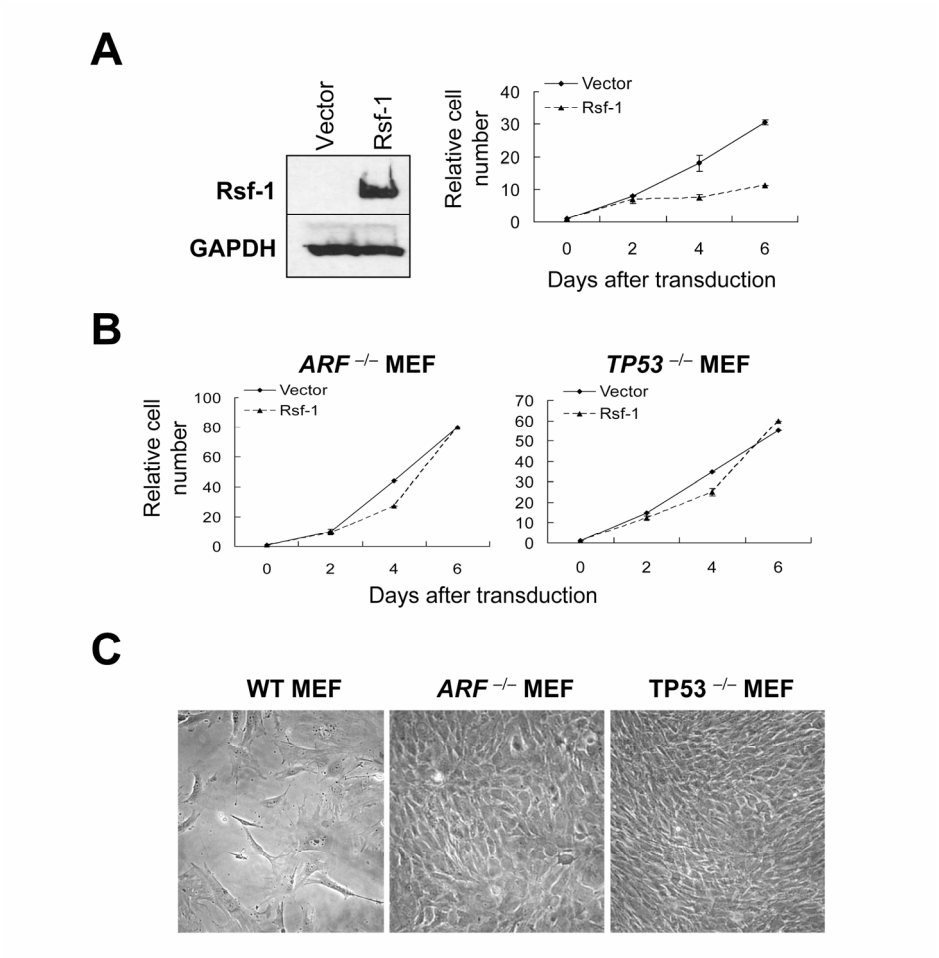
A
Vector
Rsf-1
Rsf-1
GAPDH
Relative cell number
Vector
Rsf-1
Days after transduction
B
ARF −/− MEF
TP53 −/− MEF
Relative cell number
Vector
Rsf-1
Days after transduction
C
WT MEF
ARF −/− MEF
TP53 −/− MEF

Figure 5

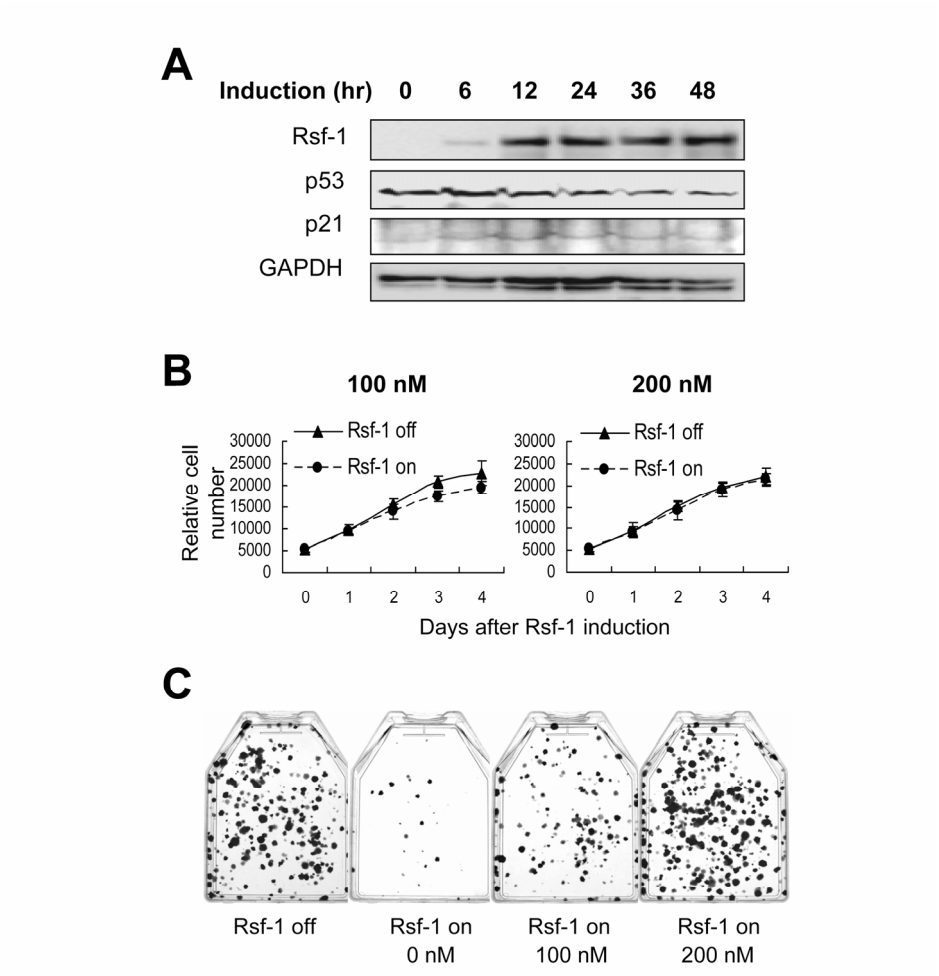
A
Induction (hr) 0 6 12 24 36 48
Rsf-1
p53
p21
GAPDH
B
100 nM
200 nM
Rsf-1 off
Rsf-1 on
Relative cell number
30000
25000
20000
15000
10000
5000
0
0 1 2 3 4
Days after Rsf-1 induction
C
Rsf-1 off
Rsf-1 on 0 nM
Rsf-1 on 100 nM
Rsf-1 on 200 nM

Figure 6

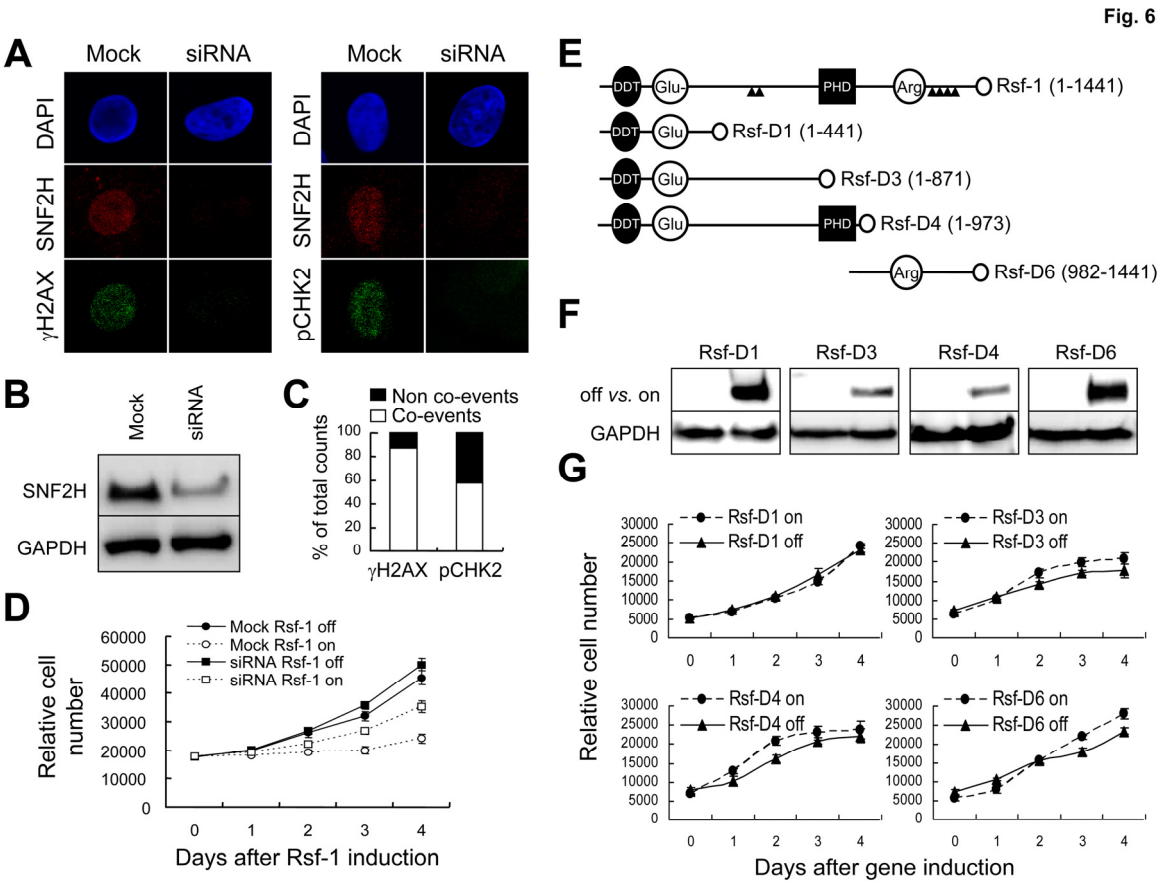
Fig. 6
A
Mock
siRNA
Mock
siRNA
DAPI
SNF2H
γH2AX
DAPI
SNF2H
pCHK2
B
Mock
siRNA
SNF2H
GAPDH
C
Non co-events
Co-events
% of total counts
100
80
60
40
20
0
γH2AX
pCHK2
D
Mock Rsf-1 off
Mock Rsf-1 on
siRNA Rsf-1 off
siRNA Rsf-1 on
Relative cell number
60000
50000
40000
30000
20000
10000
0
0
1
2
3
4
Days after Rsf-1 induction
E
DDT
Glu
PHD
Arg
Rsf-1 (1-1441)
Rsf-D1 (1-441)
Rsf-D3 (1-871)
Rsf-D4 (1-973)
Rsf-D6 (982-1441)
F
Rsf-D1
Rsf-D3
Rsf-D4
Rsf-D6
off vs. on
GAPDH
G
Rsf-D1 on
Rsf-D1 off
Rsf-D3 on
Rsf-D3 off
Rsf-D4 on
Rsf-D4 off
Rsf-D6 on
Rsf-D6 off
Relative cell number
30000
25000
20000
15000
10000
5000
0
0
1
2
3
4
Days after gene induction

Figure 7

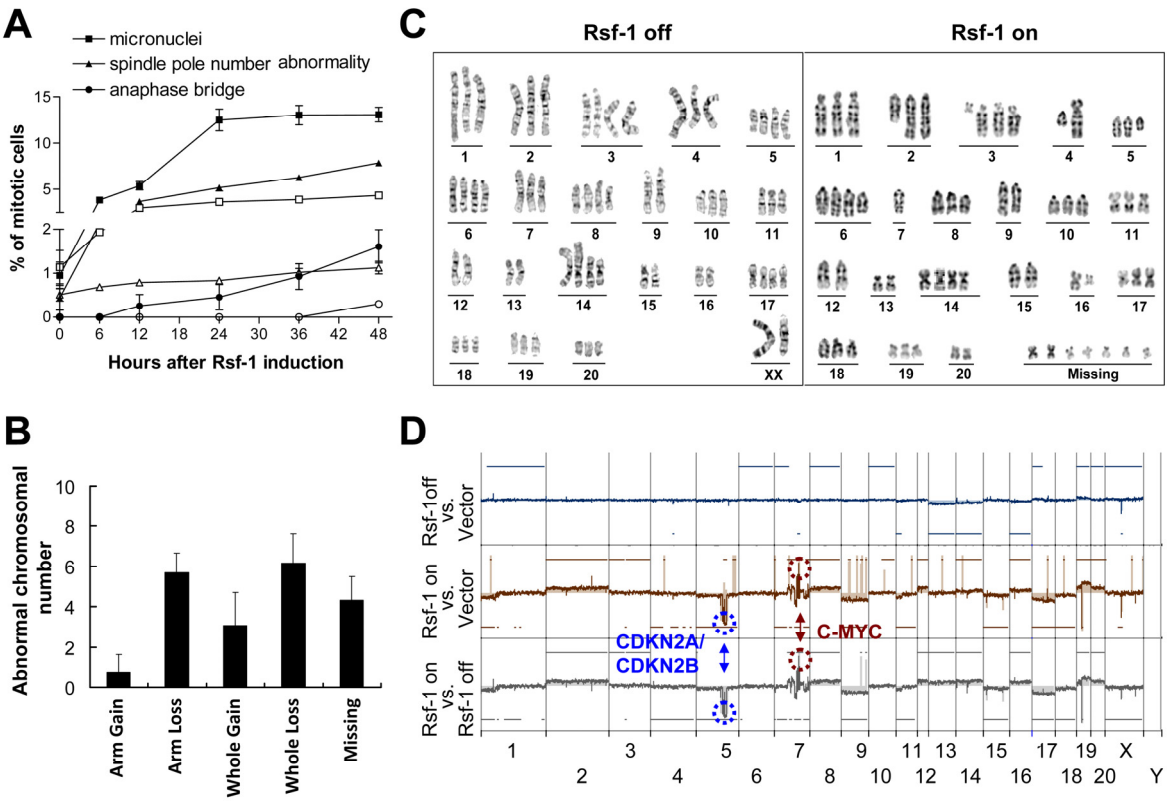
Fig. 7
A
micronuclei
spindle pole number abnormality
anaphase bridge
% of mitotic cells
Hours after Rsf-1 induction
C
Rsf-1 off
Rsf-1 on
Missing
B
Abnormal chromosomal number
Arm Gain
Arm Loss
Whole Gain
Whole Loss
Missing
D
Rsf-1off vs. Vector
Rsf-1 on vs. Vector
Rsf-1 on vs. Rsf-1 off
CDKN2A/
CDKN2B
C-MYC